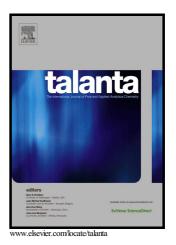# Author's Accepted Manuscript

A Sensitive Electrochemical Aptasensor for Mucin 1 Detection Based on Catalytic Hairpin Assembly Coupled with PtPdNPs Peroxidase-like Activity

Ruo-Nan Zhao, Zhe Feng, Ya-Nan Zhao, Li-Ping Jia, Rong-Na Ma, Wei Zhang, Lei Shang, Qing-Wang Xue, Huai-Sheng Wang

www.elsevier.com/locate/talanta

Cite this article as: Ruo-Nan Zhao, Zhe Feng, Ya-Nan Zhao, Li-Ping Jia, Rong-Na Ma, Wei Zhang, Lei Shang, Qing-Wang Xue and Huai-Sheng Wang, A Sensitive Electrochemical Aptasensor for Mucin 1 Detection Based on Catalytic Hairpin Assembly Coupled with PtPdNPs Peroxidase-like Activity, *Talanta,* https://doi.org/10.1016/j.talanta.2019.03.012

A Sensitive Electrochemical Aptasensor for Mucin 1 Detection Based on Catalytic Hairpin Assembly Coupled with PtPdNPs Peroxidase-like Activity

Ruo-Nan Zhao, Zhe Feng, Ya-Nan Zhao, Li-Ping Jia[1], Rong-Na Ma, Wei Zhang, Lei Shang, Qing-Wang Xue, Huai-Sheng Wang[1]

Department of Chemistry, Liaocheng University, Liaocheng, Shandong 252000, China
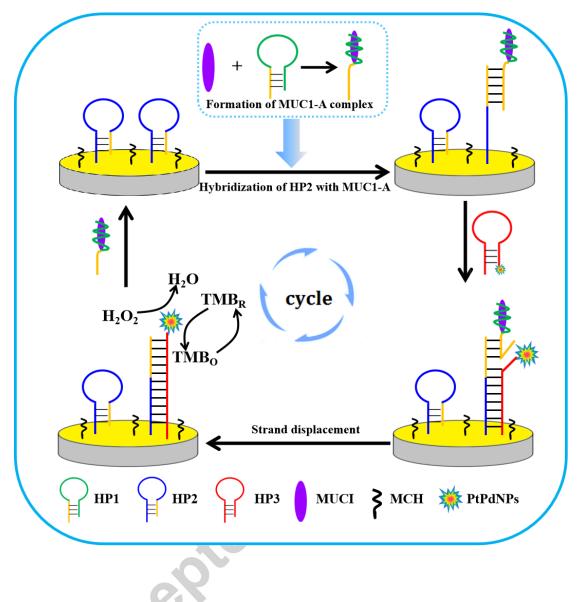
jialiping12@l63.com

hswang@lcu.edu.cn

Abstract

In this work, an ultrasensitive aptasensor for the detection of Mucin 1 (MUC1) was presented based on the target-induced catalytic hairpin assembly combined with excellent mimic peroxidase performance of PtPd bimetallic nanoparticles (PtPdNPs). Traditionally, the cyclic reuse of target protein was achieved by protein conversion with enzyme cleavage or polymerization, which is costly and complex. However, in this work, it can be performed by simple strand displacement. In addition, PtPdNPs, a mimic peroxidase, was used a probe to catalyze the oxidation of tetramethylbenzidine (TMB) by H_2O_2, leading to the electrochemical signal amplification. With this ingenious design, the prepared aptasensor for MUC1 detection showed a favorable linear response from 100 fg mL^{-1} to 1 ng mL^{-1} and a relatively low detection limit of 16 fg mL^{-1}. The proposed biosensor possessed acceptable stability, selectivity and reproducibility for MUC1 assay. Additionally, the fabricated aptasensor has been successfully applied to detect MUC1 in serum samples with satisfactory results. This new strategy supplied one efficient approach to improve signal amplification, which also open an avenue for sensitivity enhancement in targets detection.

[1] Tel: +86 0635 8239121; fax: +86 0635 8239121

Graphical abstract

Keywords: Catalytic hairpin assembly, Aptasensor, bimetallic nanoparticles, MUC1

1. Introduction

Mucins are a family of high molecular weight, heavily glycosylated proteins produced by epithelial tissues [1]. Overexpression of the mucin proteins, especially Mucin 1 (MUC1; also known as episialin, PEM, H23Ag, EMA, CA15-3, and MCA) [2], is associated with many types of cancer including breast cancer, stomach cancer, and so on [3, 4]. MUC1 is a single pass type I transmembrane protein with a heavily glycosylated extracellular domain that extends up to 200–500 nm from

the cell surface [2]. The extracellular domain of MUC1 consists of a variable number of 20 amino acid tandem repeats. Within each tandem repeat, two serines and three threonines represent five potential O-glycosylation sites that are extensively glycosylated [5]. MUC1 is normally expressed in the normal cells. However, aberrantly glycosylated MUC1 is overexpressed in most human epithelial cancers and has gained remarkable attention as an oncogenic molecule [2]. A low level of MUC1 expression (generally < 31 U mL^{-1}) could be found in healthy human serum [6]. However, the normal level of MUC1 in serum may be quite different, depending on the type of assay employed [7]. A 100-fold increase in the amount of MUC1 is indicative of greater likelihood of cancer [8]. So MUC1 can serve as a biomarker indicator for early cancer detection, and it is necessary to develop some specific and sensitive methods for MUC1 detection. Various methods such as enzyme-linked immunosorbent assay (ELISA) [9, 10], colorimetric method [11], fluorescence [12], electrochemiluminescence [13, 14] and electrochemical techniques [15-17] have been developed for MUC1 detection.

Aptamers are artificial synthetic single-stranded DNA or RNA oligonucleotides selected in vitro through a SELEX (systematic evolution of ligands by exponential enrichment) process. Aptamers can bind with various targets such as peptide, organic/inorganic molecule, protein, and cell with high specificity and affinity. Due to their versatile target binding capabilities, aptamers have attracted great attention in bioanalysis and biomedical research [18, 19]. Besides, aptamers exhibit many advantages superior to antibodies, such as ease of synthesis, high stability, low cost and easy chemical modification [20], which makes them to be a new recognition probes in designing biosensing systems. Ferreira et al. selected anti-MUC1 DNA aptamers that recognize to both a 9 amino acid immunogenic epitope of the 20 amino acid variable tandem repeat, and a 60 amino acid peptide corresponding to three copies of the 20 amino acid variable tandem repeat of MUC1 [21, 22]. The surface plasmon resonance data have confirmed the high affinity of the aptamers for the MUC1 peptides in solution. The association constant (K_a=4.01×10^6 M^{-1} s^{-1}) and dissociation constants (K_d=0.135 nM) have been obtained respectively [22]. Some aptamer-based

optical and electrochemical sensors have been reported for the detection of MUC1 [14, 17, 23]. According to the obtained data from various developed fluorescence- and luminescence-based MUC1 aptasensors, the ECL-based biosensing platforms are highly sensitive methods showing fg mL^{-1} detection limit for MUC1, whereas FRET-based aptasensors allow detecting of MUC1 at the range of nM. Acquired results of electrochemical-based aptasensors for MUC1 detection at ng mL^{-1} to pM levels are well competitive with other methods previously described [7]. However, Gupta et al. indicated that the electrochemical-based nano-aptasensors was capable of sensing concentration as low as 1 fg mL^{-1} (0.031 fM) of MUC1[24]. This is important considering that MUC1 can be found in blood in trace amounts when cancer is absent while in case of tumor development, its level rises. To further improve the sensitivity of MUC1 sensing, some signal amplification strategies such as hybridization chain reaction [25], rolling circle amplification [12] and enzyme cleavage-based signal amplification [15, 26] have been employed in the fabrication of aptasensor. However, most amplification strategies involved natural enzymes, which are expensive and need special reaction conditions. For example, nicking endonucleases are sequence-specific and thus are limited in the design of aptasensor. Fortunately, catalytic hairpin assembly (CHA), as an enzyme-free signal amplification technique with negligible background, has been engineered to initiate hundreds-fold catalytic amplification reaction [27]. Owing to the high efficiency, short analysis time and recycling of the target, the CHA-based biosensors may lead to concomitant improvements in convenience and sensitivity.

Recently, the intense interest has grown for the development of bimetallic materials-based artificial enzymes (Nanozymes) due to their superior biological enzyme-like activity [28-30]. Such nanostructures offer easy tunability to the composition and therefore, facilitate the control over the enzyme-like activity. Compared with natural enzyme, nanozymes offer better sensitivity, specificity, stability, and low cost in synthesis, purification, and storage [31]. The applications of bimetallic nanoparticles to construct the biosensors for the detection of H_2O_2, glucose and ascorbic acid have been reported [32-35].

Based on the above considerations, we developed a sensitive electrochemical aptasensor for the detection of MUC1 based on the catalytic hairpin assembly combined with excellent mimic peroxidase performance of PtPd bimetallic nanoparticles (PtPdNPs). In this study, three hairpin DNA (Apt-HP1, HP2 and HP3) were designed to fabricate the aptasensor. Firstly, Apt-HP1 containing aptamer sequence was opened only after binding with target protein to form MUC1-aptamer binding complex (abbreviated as MUC1-A), which left an exposed DNA segment to initiate CHA reaction. Next, the exposed segment of MUC1-A would attack HP2 immobilized on the electrode to form a double strand structure with a new exposed segment, which could hybridize with the toehold of PtPdNPs modified HP3. Finally, MUC1-A was released via the strand displacement process, and the released MUC1-A further participated in the subsequent reaction cycles, achieving the target recycling as well as leaving abundant PtPdNPs on the electrode. The carried PtPdNPs as mimic peroxidase could effectively catalyzed the oxidation reaction of TMB by H_2O_2 to generate redox electrochemical signals. By coupling CHA and the catalytic performance of bimetallic nanoparticles, our system provided an electrochemical detection limit of 16 fg mL^{-1}, which is 4 or 6 orders of magnitude more sensitive than those of other electrochemical methods [15, 16, 36]. The proposed scheme is simple and low cost because it is achieved only with three hairpin DNA and without any expensive enzymes being used. In addition, this strategy could be readily expanded to detect other biomolecules sensitively by changing the hairpin DNA sequences.

2. Experimental

2.1.Materials

All oligonucleotides used in the experiment were synthesized by Sangon Biotechnology Co., Ltd. (Shanghai, China), and their sequences are listed in Table S1. Human Mucin 1 (MUC1) ELISA Kit was purchased from Jianglai Biotechnology Co., Ltd (Shanghai, China). Human serum albumin (HSA), bovin serum albumin (BSA), and carcino-embryonic antigen (CEA) were purchased from Sigma-Aldrich. Tris-(2-carboxyethyl)-phosphine hydrochloride (TCEP), tris-(hydroxymethyl)-aminomethane (Tris), 6-mercapto-1-hexanol (MCH),

cetyltrimethyl ammonium bromide (CTAB), ethylenediaminetetraacetic acid (EDTA), potassium tetrachloropalladate (K_2PdCl_4), chloroplatinic acid (H_2PtCl_6), tetramethylbenzidine (TMB), hydrogen peroxide (H_2O_2), glucose, and ascorbic acid (AA) were purchased from Aladdin Inc. (Shanghai, China). All these reagents were of analytical grade and without further purification. DNA was stored in Tris-HCl (10 mM, pH 8.0) containing 1.0 mM EDTA. Tris-HCl buffer (10 mM, pH 7.4) containing 100 mM NaCl and 5 mM $MgCl_2$ was employed for hybridizing and washing. Furthermore, the thiolated HP2 and HP3 were reduced in 2 mM TCEP for 1 h to cleave disulfide bonds, respectively. Electrochemistry detection was performed in 0.1 M PBS buffer (pH 7.0) containing 0.6 mM TMB and 1.0 mM H_2O_2. All solutions were prepared with Milli-Q water (18 mΩ·cm resistivity) from a Millipore system.

2.2. Apparatus

The transmission electron microscopic (TEM) image was observed on a JEM-2100 transmission electron microscope (JEOL Ltd., Japan) with an accelerating voltage of 200 kV. X-ray diffraction (XRD) patterns were measured on Bruker D8 (with a Cu Kα radiation) instrument.

2.3. Preparation of PtPdNPs

The PtPd nanoparticles (PtPdNPs) were synthesized according to the reference [37]. First, 400 μL of 2 mM K_2PdCl_4 solution and 80 μL of 10 mM H_2PtCl_6 solution were added into 4 mL of 0.25 mM CTAB solution. Next, 2 mL of 0.1 M AA solution was added into the above solution under continuous stirring. Then, the obtained mixed solution were placed in a 30 ℃ water bath for 5 h. Finally, the as-prepared PtPdNPs were purified by centrifugation twice. The precipitates were redispersed in water for further use.

2.4. Preparation of PtPdNPs-HP3 probe

Firstly, 20 μL of HP3 (10 μM) solution were added into 200 μL PtPdNPs solutions. Then, the mixed solution was centrifuged and washed after being stirred for 24 h under 4 ℃. Finally, the obtained product was dispersed in 200 μL PBS buffer (pH 6.5).

2.5. Fabrication of the aptasensor

Firstly, a gold electrode (2 mm in diameter) was polished on a microcloth with 0.05 μm alumina slurry for 5 min, followed by sonicating in ethanol and water for 5 min, respectively. Then the polished electrode was electrochemically cleaned in 0.5 M H_2SO_4 solution by scanning from -0.3 V to +1.5 V until a steady-state cyclic voltammogram was obtained. After being thoroughly rinsed with Milli-Q water and dried with nitrogen, the cleaned electrode should be immediately used for DNA immobilization.

Prior to the fabrication of the aptasensor, the target MUC1 was first mixed with Apt-HP1 to form different concentrations of MUC1-A binding complex. As depicted in Scheme 1, 6 μL of 0.2 μM thiolated HP2 solution was first dropped on the cleaned gold electrode surface and incubated for 60 min at 37°C. Next, the electrode was immersed into 1 mM MCH for 30 min to remove the nonspecific DNA adsorption. After rinsed thoroughly and dried in nitrogen, 6 μL MUC1-A complex with different concentration was dropped on the HP1 modified electrode surface for 60 min at 37°C. Finally, 6 μL PtPdNPs-HP3 solution was dropped on the modified electrode surface to react for 60 min at 37°C. The electrode surface was washed with 10 mM Tris-HCl buffer (pH 7.4) and dried with nitrogen after each modification step.

2.6. Real sample preparation

The prepared aptasensor was also used for the analysis of real samples containing MUC1. Firstly, human serum samples (supported by Liaocheng People's Hospital) were diluted 50-fold by PBS (0.1 M, pH 7.4). Next, the diluted serums were incubated with Apt-HP1 and then performed under the same conditions as described in the Section 2.5.

2.7. Electrochemical detection

All electrochemical experiments were performed with a CHI 760C electrochemical workstation (CH Instruments, Shanghai, China) with a conventional three-electrode system comprising a gold working electrode, a platinum wire auxiliary electrode, and a Ag/AgCl reference electrode. Cyclic voltammetry (CV) and chronoamperometry were carried out in 5 mL of PBS (pH 6.5) containing 0.6 mM TMB and 1.0 mM H_2O_2 at a scan rate of 100 mV s^{-1}. Chronoamperometric response

was recorded at +450 mV. Electrochemical impedance spectroscopy (EIS) was carried out in 5 mM $[Fe(CN)_6]^{3-/4-}$ solution containing 0.1 M KCl with the frequency range from 0.1 Hz to10 kHz. The amplitude of the applied sine wave potential was 5 mV and the formal potential of the system was set at +0.22 V.

3. Results and discussion

3.1. Characterization of PtPdNPs

Fig. 1A is the TEM image of PtPdNPs. A porous branched-structure can be observed. The porous PtPdNPs have an average diameter of 35 nm. The crystallographic property of the as-synthesized bimetallic nanoparticles was examined by XRD as illustrated in Fig. 1B. The diffraction peaks around 40.24°, 46.78°, and 68.22° were observed, which corresponded to the (111), (200), and (220) planes, respectively. This result was coincident with that of the previously reported [38].

The peroxidase-like catalytic performance of PtPdNPs was evaluated with an typical colorimetric oxidation reaction of TMB by H_2O_2. As shown in Fig.2A, the mixture of TMB and H_2O_2 gave a colorless solution for a long time, indicating a slow oxidation reaction (a). Upon the addition of PtPdNPs suspension to the mixture of TMB and H_2O_2, the colorless solution turned to blue color immediately (b), indicating PtPdNPs possessed the peroxidase-like activity. Like the oxidation reaction catalyzed by peroxidase, the catalytic activity of PtPdNPs could be stopped by H_2SO_4 solution, resulting in the color change from blue to yellow (c). The catalytic performance of PtPdNPs for the oxidation of TMB by H_2O_2 was further confirmed by electrochemical measurements (Fig. 2B). TMB showed two pairs of well-defined redox peaks on bare gold electrode, which are assigned to the typical two-electron redox reaction of TMB (curve a). Compared with the CV response of TMB on bare gold electrode, the CV response on PtPdNPs modified gold electrode showed a large increase of the redox peak current (curve b), indicating the electrocatalytic ability of the immobilized PtPdNPs to the oxidation reaction of TMB by H_2O_2. Furthermore, we used the *I-t* curve to measure the current from the elecrocatalytic reaction. Obviously, an apparent increase in current was obtained on PtPdNPs modified electrode from chronoamperometric curve (Fig. 2C). This relatively large difference could make the

detection sensitive.

3.2. Design principle of MUC1 aptasensor

The design principle of the proposed MUC1 aptasensor is schematically demonstrated in Scheme 1. In the present work, three hairpin DNA probes (Apt-HP1, HP2 and HP3) were designed to fabricate the aptasensor. In the presence of target MUC1, Apt-HP1 (containing aptamer sequences) could be opened to form a MUC1-aptamer binding complex (abbreviated as MUC1-A) with an exposed segment. Next, the exposed DNA segment within MUC1-A interacted with a toehold on HP2 immobilized on gold electrode, forming a double strand structure with a new exposed segment, which could hybridize with the toehold of PtPdNPs-HP3 probe. Finally, MUC1-A was released via the strand displacement process, and the released MUC1-A further participated in the subsequent reaction cycles, achieving the target recycling as well as leaving abundant PtPdNPs on the electrode. PtPdNPs could effectively catalyzed the oxidation reaction of TMB by H_2O_2 to generate redox electrochemical signals.

3.3. Feasibility of the aptasensor

The feasibility of the proposed biosensor was confirmed by EIS and CV measurements. In a typical EIS, the diameter of semicircle equals to the electron-transfer resistance, which reflects the electron transfer kinetics of the redox probe ($[Fe(CN)_6]^{3-/4-}$) at the electrode surface. As shown in Fig. 3A, a very small semicircle was observed for bare gold electrode (curve *a*), indicating a fast electron-transfer process of $Fe(CN)_6^{3-/4-}$ redox system. The resistance increased with the immobilization of HP2 on the gold electrode surface (curve b) due to the effective repulsion between the negatively charged HP2 and $Fe(CN)_6^{3-/4-}$ anions. Subsequent surface blocking with 6-mercaptohexanol (MCH) also led to an obvious increase in resistant (curve c). After successive assembly with MUC1-A and HP3, the resistance increased gradually (curve d, e). The results indicated that the sensing interface was successfully fabricated. The electrochemical biosensor was also characterized by CV (Fig. 3B). Compared with the bare gold electrode (curve a), the peak current of the HP2 modified electrode (curve b) decreased obviously and the peak-to-peak

separation increased, which indicated that the HP2 strand was immobilized on the gold electrode surface successfully. After the surface of the HP2/Au electrode was blocked by MCH, the peak current decreased correspondingly (curve c). The peak currents further decreased (curve d, e) after incubation with MUC1-A and HP3. These results were in accordance with those observed in EIS investigation, demonstrating that the electrochemical aptasensor had been fabricated successfully according to the Scheme 1.

Then we testified the feasibility to detect target MUC1 by using this system. As shown in Fig. 3C, in the presence of MUC1 (100 pg mL^{-1}), an apparent increase in current from cyclic voltammetry was observed compared with that in the absence of MUC1. To quantify the electrochemical signal, we use the I-t curve to measure the current from the elecrocatalytic reaction. We held the potential at the catalytic oxidation potential for TMB (450 mV vs the Ag/AgCl reference electrode). In the presence of target MUC1, a decay curve for current (I) vs time (t) was observed instantly after the onset of the potential, which rapidly reached a plateau (steady-state current) within 30 s, and the steady state current was 6.5 times higher than that in the absence of target MUC1 (Fig. 3D). These results could be contributed to the fact that the MUC1 opened the hairpin structure of HP1 to form MUC1-A complex, which initiated the catalytic hairpin assembly reaction, resulting in the linkage of a great deal of PtPdNPs to the sensor surface to catalyze the oxidation of TMB by H$_2$O$_2$.

3.4. Optimization of Sensing Conditions

In order to obtain high sensitivity for target MUC1 detection, the test conditions such as the pH of reaction solution, the concentration of HP2, and the incubation time of PtPdNPs-HP3 were investigated by the aptasensor with 100 pg mL^{-1} MUC1 in 0.1 M PBS buffer containing 0.60 mM TMB and 1.0 mM H$_2$O$_2$. In this work, the fabricated aptasensor was detected in PBS buffer with different pH value. In Fig. 4A, the currents increased with the pH value increasing firstly and then decreased after the pH value was larger than 6.5. Therefore, the PBS buffer of pH 6.5 was adopted as the test solution. The concentration of HP2 immobilized on the electrode surface played an important role in this strategy. As shown in Fig.4B, the electrochemical responses

increased with the increasing concentration of HP2 up to 0.2 μM, afterward the response decreased due to the fact that the dense HP2 on sensor surface was unfavorable to its hybridization with MUCI-A. Thus, 0.2 μM HP2 was chosen for the sensor fabrication. In this study, the incubation time of PtPdNPs-HP3 caused great effect on the electrochemical response. Fig. 4C revealed the signals increased gradually from 20 to 60 min and reached a relatively stable value at 60 min. Therefore, 60 min was selected as the optimum incubation time of PtPdNPs-HP3. Furthermore, the optimization of the incubation times of HP2, MCH and MUC1-A on the electrode were also studied (shown in Fig. S1). The results indicated that the optimum incubation times were 60 min, 30 min and 60 min for HP2, MCH and MUC1-A, respectively.

3.5. Dectection of MUC1

Under optimal sensing conditions, the chronoamperometric response of the obtained sensor in 0.1 M pH 6.5 PBS buffer containing 0.6 mM TMB and 1.0 mM H_2O_2 at +450 mV increased with the increasing concentration of MUC1 (Fig. 5A). The calibration plot showed a good linear relationship between the amperometric response and the logarithm value of MUC1 concentration ranging from 100 fg mL^{-1} to 1 ng mL^{-1}. The linear equation was I (nA) = -16.556 + 21.233 log$c$ (fg mL^{-1}), (R=0.9996). The detection limit for MUC1 was estimated to be 16 fg mL^{-1} according to $3\sigma/S$, in which the σ is the standard deviation of the blank sample and S is the slope of the obtained regression equation. Compared with some previously reported methods (Table S2), the proposed aptasensor exhibited broader linear range as well as a relatively low detection limit for MUC1 determination. The high sensitivity of this aptasensor may be ascribed to the target recycling for signal amplification.

3.6. Selectivity, reproducibility and stability of the proposed aptasensor

Some important performances, such as selectivity, stability, and reproducibility of this proposed biosensor were investigated. Specificity is one of the most significant factors for evaluating a detection system. To assess the specificity of the aptasensor, some proteins including bovine serum albumin (BSA), human serum albumin (HSA), carcinoembryonic antigen (CEA) and glucose were tested at concentrations of 10 μg

mL^{-1}, while the concentration of MUC1 was 100 pg mL^{-1}. As shown in Fig. 6, MUC1 showed a much stronger response compared to the other proteins. In addition, the current response of MUC1 in the presence of these interfering materials were similar to that without interferent. However, the concentration of HSA in real human serum samples is very high, so we also studied the effect of higher concentration of HSA on the detection of low level MUC1. The results showed that the current responses of 10 pg mL^{-1} MUC1 coexisting with 0.01 mg mL^{-1}, 0.1 mg mL^{-1}, and 1.0 mg mL^{-1} HSA decreased slightly compared with that only in the presence of MUC1. However, the current responses decreased significantly when HSA concentrations were above 5 mg mL^{-1} (shown in Fig. S2). Therefore, in the potential application for analysis of real blood serum samples, the samples should be diluted to a certain times to eliminate the interference of HSA.

The reproducibility was assessed by assaying the same concentration of MUC1 with five different aptasensors prepared independently at the same experimental conditions. The relative standard deviations (RSD) for the parallel detection of 100 pg mL^{-1} and 10 pg mL^{-1} MUC1 with 5 different aptasensors were 4.82% and 6.32%, respectively. Furthermore, 100 pg mL^{-1} and 10 pg mL^{-1} MUC1 was tested by one aptasensor for five times with RSD of 3.26% and 5.34%, respectively. The results implied an acceptable reproducibility for determination of MUC1. The prepared aptasensor was kept at 4 ℃ and tested each day. After stored for a week, the electrochemical signal maintained 92.8% of its original current response, showing that the prepared aptasensor had satisfactory stability. As a consequence, the proposed biosensor possessed excellent stability, selectivity and reproducibility for MUC1 assay.

3.7. Application of the aptasensor in Human Serum

To evaluate the applicability of the proposed aptasensor, the aptasensor was applied to detect MUC1 in the complicated sample matrix by adding different concentrations of standard MUC1 into human serum (supported by Liaocheng People's Hospital, 50-fold-diluted before use). The concentrations of MUC1 in the diluted samples obtained by the proposed electrochemical aptasensor and those obtained by ELISA

were listed in Table 1. The results indicated the relative errors were at an acceptable and satisfactory range. Therefore, the proposed aptasensor for MUC1 detection was reliable and practical in clinical determination of MUC1.

4. Conclusion

In summary, a new strategy for the electrochemical detection of target MUC1 based on catalytic hairpin assembly combined with the electrocatalytic activity of bimetallic nanoparticles was developed. The multiple use of target MUC1 was simply achieved by strand displacement reaction without involving expensive nature enzyme and complicated procedures. Furthermore, bimetallic nanoparticles PtPdNPs as artificial enzyme possessed high electrocatalytic ability to the oxidation of TMB by H_2O_2, which led to a high sensitivity for the proposed biosensor. Compared with reported electrochemical methods for the detection of MUC1, the proposed scheme was simple because just three hairpin DNA probes are introduced. Furthermore, the assay time of the aptasensor was about 4 h, which was less than those reported electrochemical methods [39, 40]. Benefiting from the target cycling amplification strategy and the excellent electrocatalytic ability of PtPdNPs, the aptasensor showed a high sensitivity for MUC1 detection with a low detection limit of 16 fg mL^{-1}. In addition, this strategy could be readily expanded to detect other biomolecules sensitively by changing the hairpin DNA sequences.

Reference

[1] F. Marin, G. Luquet, B. Marie, D. Medakovic, Molluscan shell proteins: primary structure, origin, and evolution, Curr. Top. Dev. Biol. 80 (2007) 209–276.

[2] S. Nath, P. Mukherjee, MUC1: a multifaceted oncoprotein with a key role in cancer progression, Trends Mol. Med. 2014 (20) 332-342.

[3] Y. Niv, MUC1 and colorectal cancer pathophysiology considerations, World J Gastroentero. 14 (2008): 2139–2141.

[4] D.W. Kufe, Mucins in cancer: function, prognosis and therapy, Nat. Rev. Cancer. 9 (2009) 874-885.

[5] C.H.M.J.Van Elssen, H.Clausen, W.T.V. Germeraad, E.P. Bennet, P.P. Menheere, G.M.J. Bos, J.Vanderlocht, Flow cytometry-based assay to evaluate human serum MUC1-Tn antibodies, J. Immunol. Methods, 365 (2011) 87-94.

[6] M.S. Nabavinia, A. Gholoobi, F. Charbgoo, M. Nabavinia, M. Ramezani, K. Abnous, Anti- MUC1 aptamer: A potential opportunity for cancer treatment, Med. Res. Rev. 37 (2017) 1518-1539.

[7] M. Yousefi, S. Dehghani, R. Nosrati, H. Zare, M. Evazalipour, J. Mosafer, B.S. Tehrani, A. Pasdar, A. Mokhtarzadeh, M. Ramezani, Aptasensors as a new sensing technology developed for the detection of MUC1 mucin: A review, Biosens. Bioelectron. 130 (2019) 1-19.

[8] E. Gheybi, J. Amani, A.H. Salmanian, F. Mashayekhi, S. Khodi, Designing a recombinant chimeric construct contain MUC1 and HER2 extracellular domain for prediagnostic breast cancer, Tumor Biology. 35 (20141) 11489-11497.

[9] R. Falahat, M. Wiranowska, N.D. Gallant, D. Toomey, R. Hill, R. Alcantar, N. A cell ELISA for the quantification of MUC1 mucin (CD227) expressed by cancer cells of epithelial and neuroectodermal origin, Cell. Immunol. 298 (2015) 96-103.

[10] C.S.M. Ferreira, K. Papamichael, G. Guilbault, T. Schwarzacher, J. Gariepy, S. Missailidis, DNA aptamers against the MUC1 tumour marker: design of aptamer–antibody sandwich ELISA for the early diagnosis of epithelial tumours, Anal. Bioanal. Chem. 390 (2008) 1039-1050.

[11] S.W. Liu, N.H. Xu, C.Y. Tan, W. Fang, Y. Tan, Y.Y. Jiang, A sensitive

colorimetric aptasensor based on trivalent peroxidasemimic DNAzyme and magnetic nanoparticles, Anal. Chim. Acta. 1018 (2018) 86-93.

[12] W.T. Yang, Y. Shen, D. Zhang, W.J. Xu, Protein-responsive rolling circle amplification as a tandem template to drive amplified transduction of fluorescence signal probes for highly sensitive immunoassay, Chem. Commun. 54 (2018) 10195-10198.

[13] X. Jiang, H. Wang, H. Wang, Y. Zhuo, R. Yuan, Y. Chai, Electrochemiluminescence biosensor based on 3-D DNA nanomachine signal probe powered by protein-aptamer binding complex for ultrasensitive Mucin 1 detection, Anal. Chem. 89 (2017) 4280-4286.

[14] X.Y. Jiang, H.J. Wang, H.J. Wang, R. Yuan, Y.Q. Chai. Signal-switchable electrochemiluminescence system coupled with target recycling amplification strategy for sensitive mercury ion and Mucin 1 assay, Anal. Chem. 88 (2016) 9243-9250.

[15] C.Y. Lin, H.X. Zheng, Y.Y. Huang, R. Yuan, Y. Q. Chai. Homogeneous electrochemical aptasensor for mucin 1 detection based on exonuclease I-assisted target recycling amplification strategy, Biosens. Bioelectron. 117 (2018) 474-479.

[16] A.E. Karpik, B.P. Crulhas, C.B. Rodrigues, Z.L. Chen, F. Luo, J. Wang, L.H. Guo, B. Qiu, Z.Y. Lin, H.H. Yang, Aptamer- based biosensor developed to monitor MUC1 released by prostate cancer cells, Electroanalysis. 29 (2017) 2246-2253.

[17] R. Hu, W. Wen, Q. Wang, G.R. Castro, V.A. Pedrosa, Novel electrochemical aptamer biosensor based on an enzyme–gold nanoparticle dual label for the ultrasensitive detection of epithelial tumour marker MUC1, Biosens. Bioelectron. 53 (2014) 384–389.

[18] E.J. Cho, J.W. Lee, A.D. Ellington, Q. Wang, H. Xiong, X. Zhang, H. Gu, S. Wang, Applications of aptamers as sensors, Annu. Rev. Anal. Chem. 2 (2009) 241–264.

[19] T. Chen, M.I. Shukoor, Y. Chen, Q. Yuan, Z. Zhu, Z.L. Zhao, B. Gulbakan, W.H. Tan, Aptamer-conjugated nanomaterials for bioanalysis and biotechnology

appli-cations, Nanoscale. 3 (2011) 546–556.

[20] T. Hianik, J. Wang, Electrochemical aptasensors—recent achievements and per-spectives, Electroanal. 21 (2009) 1223–1235.

[21] A. K. H. Cheng, H.P. Su, Y. A. Wang, H.Z. Yu, Aptamer-Based Detection of Epithelial Tumor Marker Mucin 1 with Quantum Dot-Based Fluorescence Readout, Anal. Chem. 81 (2009) 6130-6139.

[22] C.S.M. Ferreira, C.S. Matthews, S. Missailidis, DNA Aptamers That Bind to MUC1 Tumour Marker: Design and Characterization of MUC1-Binding Single-Stranded DNA Aptamers, Tumor Biol. 27 (2006) 289-301.

[23] Y. He, Y. Lin, H.W. Tang, D.W. Pang, A graphene oxide-based fluorescent aptasensor for the turn-on detection of epithelial tumor marker mucin1, Nanoscale. 4 (2012) 2054-2059.

[24] P. Gupta, A. Bharti, N. Kaur, S. Singh, N. Prabhakar, An electrochemical aptasensor based on gold nanoparticles and graphene oxide doped poly(3,4-ethylenedioxythiophene) nanocomposite for detection of MUC1. J. Electroanal. Chem. 813 (2018) 102-108.

[25] C. Ma, H.Y. Liu, T. Tian, X.R. Song, J.H. Yu, M. Yan, A simple and rapid detection assay for peptides based on the specific recognition of aptamer and signal amplification of hybridization chain reaction, Biosens. Bioelectron. 83 (2016) 15–18.

[26] W. Wen, R. Hu, T. Bao, X.H. Zhang, S.F. Wang, An insertion approach electrochemical aptasensor for mucin 1 detection based on exonuclease-assisted target recycling, Bionses. Bioelectron. 71 (2015) 13-17.

[27] Y. Jiang, B.L Li, J.N. Milligan, S. Bhadra, A.D. Ellington, Real-time detection of isothermal amplification reactions with thermostable catalytic hairpin Assembly, J. Am. Chem. Soc. 135 (2013) 7430–7433.

[28] Y. Lu, W. Ye, Q. Yang, J. Yu, Q. Wang, P. Zhou, C. Wang, D. Xue, S. Zhao, Three-dimensional hierarchical porous PtCu dendrites: a highly efficient peroxidase nanozyme for colorimetric detection of H_2O_2, Sens. Actuators B: Chem. 230 (2016) 721-730.

[29] L. Li, C. Zeng, L. Ai, J. Jiang, Synthesis of reduced graphene oxide-iron nanoparticles with superior enzyme-mimetic activity for biosensing application, J. Alloy. Compd. 639 (2015) 470-477.

[30] Y. Lin, J. Ren, X. Qu, Catalytically active nanomaterials: a promising candidate for artificial enzymes, Acc. Chem. Res. 47 (2014) 1097-1105.

[31] K.J. Shah, S.T. Bhagat, D. Varade, S. Singh, Novel synthesis of polyoxyethylene cholesteryl ether coated Fe-Pt nanoalloys: A multifunctional and cytocompatible bimetallic alloy exhibiting intrinsic chemical catalysis and biological enzyme-like activities, Colloids and Surfaces A: Physicochemical and Engineering Aspects, 553 (2018) 50-57.

[32] M. Janyasupab, C.W. Liu, Y. Zhang, K.W. Wang, C.C. Liu, Bimetallic Pt–M (M = Cu, Ni, Pd, and Rh) nanoporous for H_2O_2 based amperometric biosensors, Sens. Actuators B: Chem. 179 (2013) 209-214.

[33] X. Zhang, Y. Cao, S. Yu, F.C. Yang, P.X. Xi, An electrochemical biosensor for ascorbic acid based on carbon-supported Pd Ninanoparticles, Biosens. Bioelectron. 44 (2013) 183-190.

[34] C.C. Shen, J. Su, X.Z. Li, J.J Luo, M.H. Yang, Electrochemical sensing platform based on Pd–Au bimetallic cluster for non-enzymatic detection of glucose, Sens. Actuators B: Chem. 209 (2015) 695-700.

[35] X.M. Chen, B.Y. Su, Z.X. Cai, X. Chen, M. Oyama, PtPd nanodendrites supported on graphene nanosheets: A peroxidase-like catalyst for colorimetric detection of H_2O_2, Sens. Actuators B: Chem. 201 (2014) 286-292.

[36] C.Y. Deng, X.M. Pi, P. Qian, X.Q. Chen, W.M. Wu, J. Xiang, High-performance ratiometric electrochemical method based on the combination of signal probe and inner reference probe in one hairpin-structured DNA, Anal. Chem. 89 (2017) 966-973.

[37] W.W. He, X.C. Wu, J.B. Liu, X.N. Hu, K. Zhang, S. Hou, W.Y. Zhou, S.S. Xie, Design of AgM bimetallic alloy nanostructures (M=Au, Pd, Pt) with tunable morphology and peroxidase-like activity, Chem. Mater. 22 (2010) 2988–2994.

[38] K. Fu, Y. Wang, L.C. Mao, X.X. Yang, J.H. Jin, S.L. Yang, G. Li, Facile

morphology controllable synthesis of PtPd nanorods on graphene-multiwalled carbon nanotube hybrid support as efficient electrocatalysts for oxygen reduction reaction, Mater. Res. Bull. 108 (2018) 187–194.

[39] S.K. Li, A.Y. Chen, Y.Q. Chai, R. Yuan, Y. Zhuo, Electrochemiluminescence aptasensor based on cascading amplification of nicking endonuclease-assisted target recycling and rolling circle amplifications for Mucin 1 detection, Electrochim. Acta. 212 (2016) 767–774.

[40] X. Liu, Y. Qin, C.Y. Deng, J. Xiang, Y.J. Li, A simple and sensitive impedimetric aptasensor for the detection of tumor markers based on gold nanoparticles signal amplification, Talanta, 132 (2015) 150–154.

Fig. 1. The TEM image (A) and XRD pattern (B) of PtPdNPs.

Fig. 2. (A) Photograph of (a) the mixtures of TMB and H_2O_2, (b, c) the mixtures of TMB, H_2O_2, and PtPdNPs before (b) and after (c) adding H_2SO_4. (B) CVs and (C) I-t curves of bare gold electrode (a) and PtPdNPs modified gold electrode (b) in 0.1 M PBS (pH 6.5) containing 0.6 mM TMB and 1.0 mM H_2O_2.

Fig. 3. (A) and (B) are EIS and CVs response of bare gold electrode (a), HP2/Au (b), MCH/HP2/Au (c), MUC1-A/MCH/HP2/Au (d), PtPdNPs-HP3/MUC1-A/MCH/HP2/Au (e) in 5 mM $[Fe(CN)_6]^{3-/4-}$ solution. (C) and (D) are the CVs and I-t curves of the proposed aptasensor in the absence (a) and presence (b) of 100 pg mL^{-1} MUC1 in 0.1 M PBS (pH 6.5) containing 0.6 mM TMB and 1.0 mM H_2O_2. Scanrate: 100 mV s^{-1}; Potential: +450 mV.
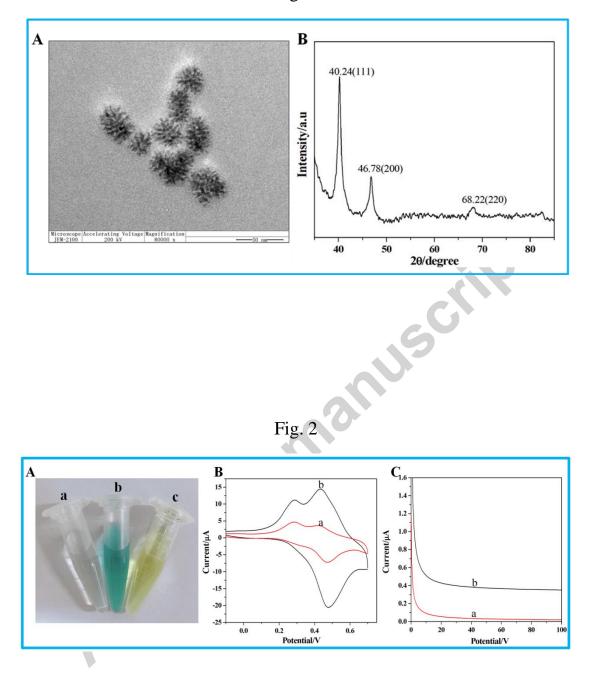
Fig. 4. Effects of (A) pH of detection solution, (B) HP2 concentration, and (C) incubation time of PtPdNPs-HP3 on CV response to 100 pg mL^{-1} MUC1. Error bars represent standard deviations for three independent experiments.

Fig. 5. (A) Chronoamperometric detection of MUC1at different concentrations at +450 mV. (B) plot of current at 100 s vs logarithmic of MUC1 concentration. Error bars show the standard deviations for three independent experiments.

Fig. 6. Specificity of the proposed biosensor toward different interfering substances. The concentration of MUC1 was 100 pg mL^{-1}, the concentrations of interfering substances were 10 μg mL^{-1}.

Scheme 1. Schematic representation of the aptasensor for the detection of MUC1.
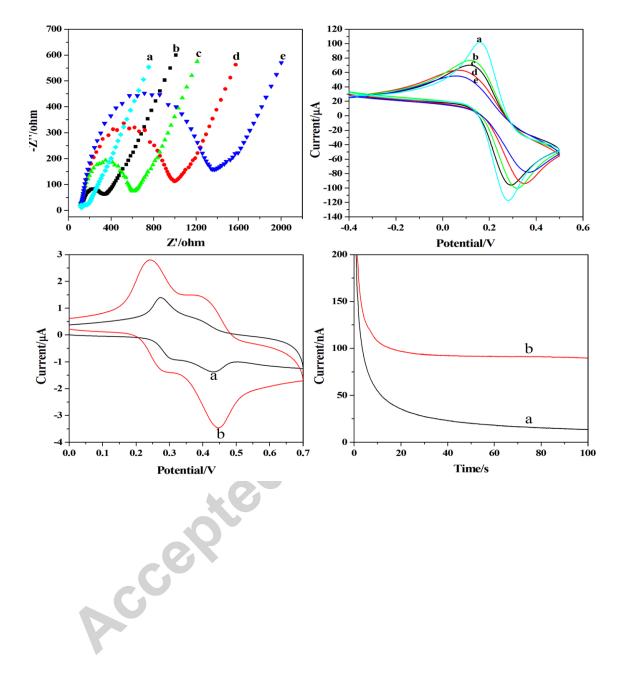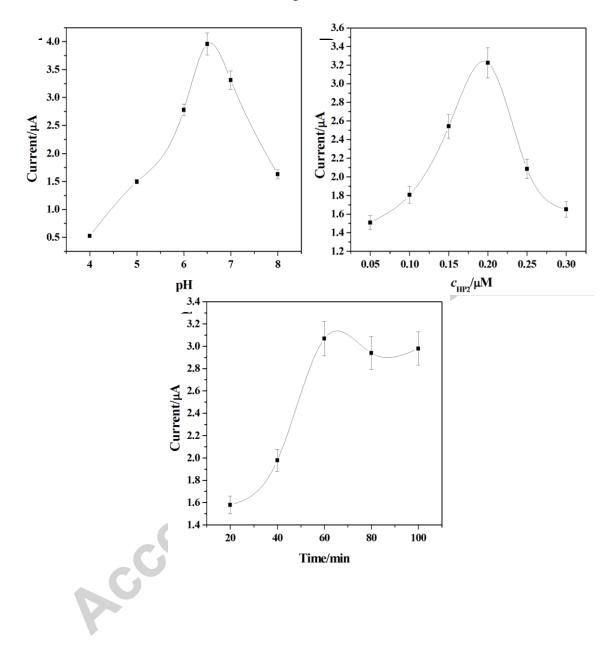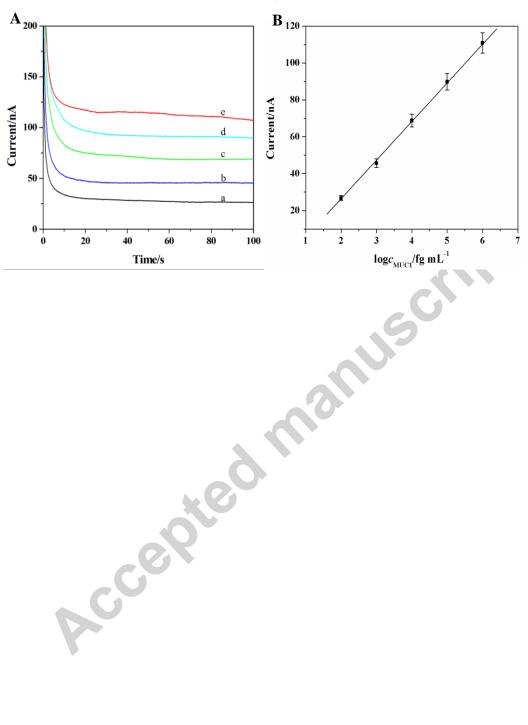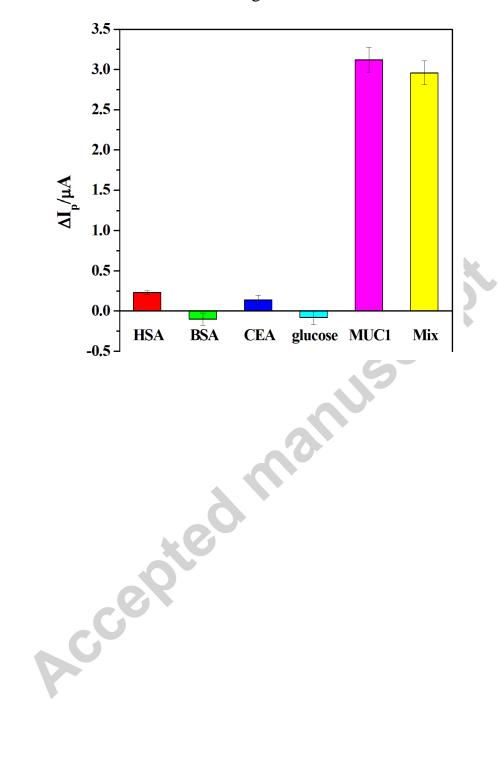
Fig. 1

Fig. 2

Fig. 3

Fig. 4

Fig. 5

Fig. 6

Scheme 1

Table 1. Detection of MUC1 in human serum samples with proposed method (n=3)

Sample	Detected (ng mL^{-1})	ELISA (ng mL^{-1})	Relative error (%)	RSD (%)
1	0.44	0.48	-8.33	3.24
2	0.66	0.71	-7.04	5.70

Highlight:

- An aptasensor based on catalytic hairpin assembly and target recycling amplification.

- PtPd bimetallic nanoparticles with mimic peroxidase performance was used as probe.

- This aptasensor was simplicity, and high sensitivity.